

# A theory for the free shrinkage of steel fibre reinforced cement matrices

P. S. MANGAT, M. MOTAMEDI AZARI

*Department of Engineering, University of Aberdeen, Marischal College, Aberdeen AB9 1AS, UK*

The paper presents a theoretical model to predict the free shrinkage of cement matrices reinforced with randomly oriented discrete steel fibres. The model is based on the consideration that the equivalent aligned length of a random fibre is responsible for restraining the shrinkage of a thick matrix cylinder of diameter equal to the fibre spacing, through the fibre–matrix interfacial bond strength. The validity of the model is established by means of extensive experimental data for different types of steel fibres in cement, mortar or concrete matrices. The theoretical model is also used to determine the values of coefficient of friction,  $\mu$ , and the average bond strength,  $\tau$ , of the fibre–matrix interface. It is shown that  $\mu$  is a basic property of the matrix and fibre interface, which is affected by the surface roughness and mechanical deformation of the fibres.  $\tau$ , however, is greatly influenced by the shrinkage of the matrix and volume fraction of fibres. Finally, an empirical expression is derived to determine the shrinkage of steel fibre reinforced cement matrices based on the shrinkage of unreinforced matrices and fibre properties.

## 1. Introduction

The restraint provided by aggregate particles to the shrinkage of concrete is well recognized. Theoretical models have been successfully developed [1] but precise design expressions are not possible largely due to the irregular geometry of aggregate particles and their variable physical and mechanical properties. The restraint to shrinkage is primarily due to the difference in the stiffness of the aggregate particles and cement matrices, where idealized spherical aggregate inclusions restrain deformations in a radial direction.

Although there are many similarities between the effect of steel fibres and aggregates on the deformation characteristics of cement matrices, the long, thin shape of the fibres leads to some fundamental differences. The contact area at the tip of a fibre is too small for the matrix to transfer any significant force in the fibre, and therefore there is little restraint to the deformation of the matrix parallel to the fibre, due to strain compatibility. The shrinking matrix, in fact, has a tendency to slide past the length of the fibre and restraint

is only possible through the fibre–matrix interfacial bond strength.

A shrinkage model for cement matrices reinforced with randomly oriented short steel fibres is proposed in this paper, based on the concepts introduced above. Experimental data using crimped, melt extract, hooked and plain steel fibres in cement, mortar and concrete matrices are used to verify the validity of the theory.

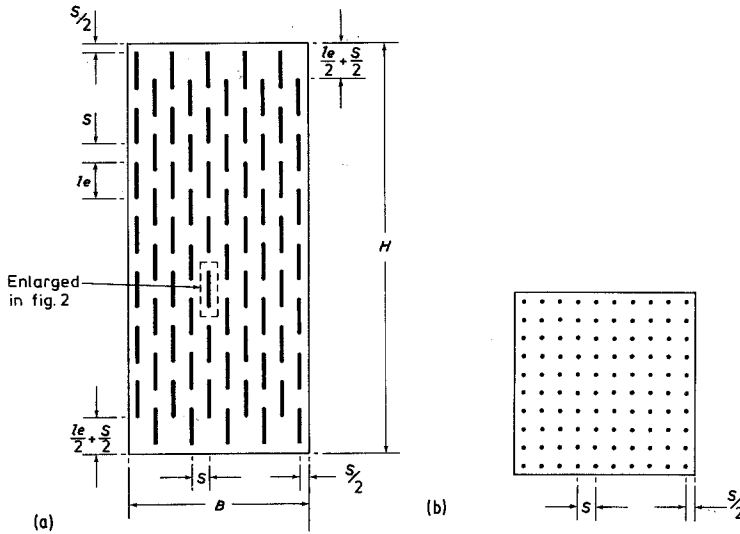
A simple empirical expression to predict the shrinkage of steel fibre reinforced cement matrices is also derived, based on the extensive shrinkage data presented in this paper.

## 2. Free shrinkage theory

### 2.1. Spacing of fibres

The distribution of randomly oriented fibres of length  $l$  and volume  $V_f$  in cementitious matrices is assumed to be represented in an idealized form by aligned fibres of effective length  $l_e$  at a spacing  $s$  as shown in Figs. 1a and b. The total length,  $L$ , of an imaginary continuous fibre which would be produced by volume  $V_f$  of randomly oriented

Figure 1 Idealized fibre distribution.



discrete fibres of diameter  $d$  is given by:

$$L = \frac{V_f}{\pi d^2/4} \quad (1)$$

The value of  $V_f$  adopted is relative to the mortar constituents of a mix, the volume of coarse aggregate being excluded.

Assuming the orientation factor of the randomly oriented fibres to be 0.41 [2], and referring to Figs. 1a and b for the definition of symbols, the following expressions can be formulated:

$$\text{Effective length, } l_e = 0.41l \quad (2)$$

$$n \times 0.41l \times N^2 = 0.41L \quad (3)$$

$$n \times 0.41l + ns + 0.41 \frac{l}{2} = H \quad (4)$$

$$Ns = B \quad (5)$$

where  $n$  is the number of fibres in one column across the prism height in Fig. 1a and  $N$  is the number of fibres in one row in the cross-section of the prism in Fig. 1b.

A solution of Equations 3, 4 and 5 leads to

the following expression which is used to calculate spacing between fibres:

$$s^3 + 0.41ls^2 - B^2 \left( H - \frac{0.41l}{2} \right) \frac{l}{L} = 0 \quad (6)$$

## 2.2. Free shrinkage model

The section within the dotted area in Fig. 1a is enlarged in Fig. 2 to present a shrinkage model for cement-based matrices reinforced with randomly oriented steel fibres. Each steel fibre, as shown in Fig. 2, is considered to reinforce a cylindrical zone of the matrix of diameter  $s$  and length  $(l_e + s)$  when  $l_e$  is the effective length of a single fibre and  $s$  is the spacing between fibres. The shrinkage of the cylindrical matrix which is adjacent to the fibre is considered to be influenced by the fibre, whereas the top and bottom parts of length  $s/2$  each are assumed to be free of the fibre influence.

The shrinkage of the matrix in any direction is considered to be restrained by an aligned fibre of effective length  $l_e$  parallel to the direction of the shrinkage strain. This is due to the tendency

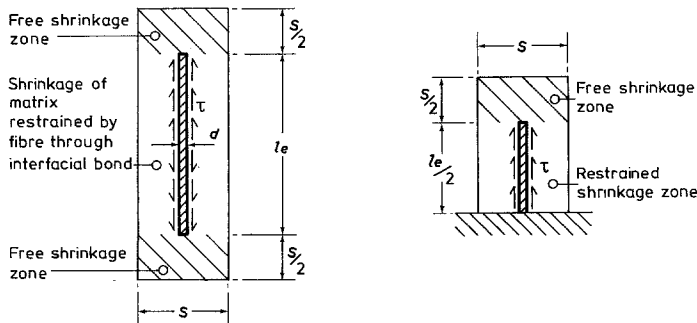


Figure 2 Shrinkage model for fibre reinforced cement matrices.

of the matrix to slide past the fibre during shrinkage, the fibre in turn providing restraint to the sliding action through the fibre–matrix interfacial bond strength.

### 2.3. Theoretical expression for free shrinkage

An expression for the free shrinkage of steel fibre reinforced cement matrices is obtained from the model shown in Fig. 2 in terms of the free shrinkage of the unreinforced control matrix and the restraint provided by the interfacial bond against the sliding action of the matrix relative to the fibre. These considerations lead to the following expression for the free shrinkage of steel fibre reinforced matrices:

$$\epsilon_{fs} \left( 0.41 \frac{l}{2} + \frac{s}{2} \right) = \epsilon_{os} \left( 0.41 \frac{l}{2} + \frac{s}{2} \right) - \tau \pi d \times 0.41 \frac{l}{2} \times 0.41 \frac{l}{2} \times \frac{1}{AE} \quad (7)$$

where  $\epsilon_{fs}$  is the shrinkage strain of fibre reinforced matrices;  $\epsilon_{os}$  is the shrinkage strain of unreinforced control matrices;  $\tau$  is the average fibre–matrix interfacial bond strength;  $E$  is the elastic modulus of the matrix;  $A$  is the area of the cylindrical matrix around a single fibre (Fig. 3a) which equals  $\pi s^2/4$ .

Equation 7 can be simplified to give the following expression for shrinkage:

$$\epsilon_{fs} = \epsilon_{os} - \frac{0.3362\tau d l^2}{s^2 E (0.41l + s)} \quad (8)$$

The solution of the above equation requires a knowledge of  $\tau$  which is derived in the preceding sections.

### 2.4. Determination of the coefficient of friction, $\mu$

The shrinkage of a cement matrix occurs in all directions. The effect of shrinkage in a lateral direction to the axis of a fibre is shown in Fig. 3. The net lateral shrinkage strains of the matrix cylinder exert a radial pressure,  $P$ , on the fibre surface as shown in Fig. 3b. The product of this radial pressure and the coefficient of friction,  $\mu$ , between the fibre and the matrix gives the magnitude of the average fibre–matrix interfacial bond strength,  $\tau$ .

The steel fibre in turn restrains the lateral deformation of the matrix cylinder due to pressure  $P$ . The value of this pressure is calculated by considering the fibre to cause a virtual radial deformation equal to the free unrestrained radial shrinkage of the matrix cylinder,  $u_m$ , minus the radial deformation of the fibre itself,  $u_f$ , under pressure  $P$ . Hence the virtual radial deformation of the matrix,  $u$ , can be expressed as:

$$u = u_m - u_f \quad (9)$$

The magnitude of the radial deformation of the cylindrical matrix surrounding a single fibre, in the absence of any restraint by the fibre is given as:

$$u_m = \epsilon_{os} \left( \frac{s}{2} - \frac{d}{2} \right) \quad (10)$$

assuming the free shrinkage of the control matrix,  $\epsilon_{os}$ , to be uniform throughout the cylindrical matrix.

The radial deformation of a fibre under pressure,  $P$ , can be obtained from the following equation which is based on Lamé's equation for solid cylinders [3]:

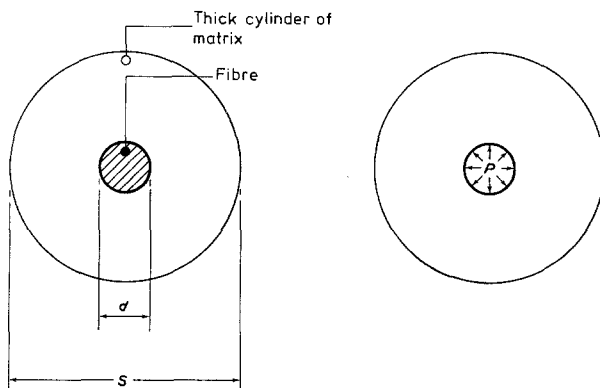


Figure 3 State of radial stress in shrinkage model.

$$u_f = \frac{P(d/2)}{E_s} (1 - \nu_s) \quad (11)$$

where  $P$  is the radial pressure;  $E_s$  is the Young's modulus of steel, assumed to be  $200 \text{ kN mm}^{-2}$ ;  $\nu_s$  is the Poisson's ratio of steel fibres which is assumed to equal 0.3.

Based on Lamé's equations for thick cylinders [3] under internal radial pressure,  $P$  (Fig. 3b), the following expression for  $u$  in terms of  $P$  can be derived:

$$u = \frac{P(d/2)}{E} \left[ \frac{(s/2)^2 + (d/2)^2}{(s/2)^2 - (d/2)^2} + \nu \right] \quad (12)$$

where  $E$  is the elastic modulus of cement matrices and  $\nu$  is the Poisson's ratio of cement matrices which is assumed to equal 0.2.

Substituting in Equation 9 for  $u$ ,  $u_m$  and  $u_f$  from Equations 12, 10 and 11, respectively, gives:

$$\frac{P}{E} = \frac{\epsilon_{os}[(s/2) - (d/2)]}{(d/2)} \times \left\{ \left[ \frac{(s/2)^2 + (d/2)^2}{(s/2)^2 - (d/2)^2} + \nu \right] + \frac{(1 - \nu_s)}{E_s/E} \right\}^{-1} \quad (13)$$

An expression for the coefficient of friction,  $\mu$ , can hence be obtained by dividing  $\tau/E$  from Equation 7 by  $P/E$  from Equation 13 to give:

$$\mu = \frac{\tau}{P} = \frac{(\epsilon_{os} - \epsilon_{fs}) \left( 0.41 \frac{l}{2} + \frac{s}{2} \right) A}{\pi d \left( 0.41 \frac{l}{2} \right)^2} \times \frac{\left\{ \left[ \frac{(s/2)^2 + (d/2)^2}{(s/2)^2 - (d/2)^2} + \nu \right] + \frac{(1 - \nu_s)}{E_s/E} \right\} \frac{d}{2}}{\epsilon_{os} \left( \frac{s}{2} - \frac{d}{2} \right)} \quad (14)$$

By using the experimental data obtained in this investigation, values of pressure,  $P$ , and coefficient of friction,  $\mu$ , are determined from Equations 13 and 14 respectively. The fibre-matrix interfacial bond values are then determined by the expression

$$\tau = \mu P \quad (15)$$

These  $\tau$  values are substituted in Equation 8 to determine the shrinkage strain of steel fibre reinforced cement based materials.

### 3. Experimental programme

Details of the experimental programme are given in Table I. The mix proportions used in this investigation are 1:1.5:2.2:0.54 and 1:2.5:1.2:0.58 for concrete, 1:2.75:0:0.58 for mortar and 1:0:0:0.35 for cement-paste. The materials used were Ordinary Portland Cement, washed sand conforming to zone 2 of BS 882 and coarse aggregate of 10 mm nominal size in accordance with BS 442. Different types of steel fibres were used namely crimped, hooked and melt extract. Details of the fibres are given in Table I.

Prism specimens of size  $100 \text{ mm} \times 100 \text{ mm} \times 500 \text{ mm}$  were cast in three layers, each layer being compacted on a vibrating table for a few seconds. The prisms were then covered with a polythene sheet for 24 h. Subsequently all the specimens, except for concrete prisms reinforced with hooked fibres, were transferred to the temperature and humidity controlled room where a temperature of  $20^\circ \text{C}$  and relative humidity of 55 per cent was maintained throughout (Table I). The prisms reinforced with hooked fibres together with their control specimens, were cured in the laboratory

TABLE I Experimental programme

Mix	Mix proportions	Fibre details				Remarks
		$l$ (mm)	Equivalent $d$ (mm)	$V_f$ (%)	Fibre type	
$A_c$	1:2.5:1.2:0.58	48.7	1.14	1, 2, 3	Crimped	Controlled curing conditions
$A_m$		22.5	0.40	1.5, 3	Melt extract	
$A_h$		28.2	0.48	1, 2	Hooked	Uncontrolled curing conditions
$A_o$		—	—	0	—	Controlled curing conditions
$B_h$	1:1.5:1.2:0.54	28.2	0.48	2	Hooked	Uncontrolled curing conditions
$B_o$		—	—	0	—	
$M_h$	1:2.75:0:0.58	28.2	0.48	3	Hooked	Controlled curing conditions
$M_m$		22.5	0.40	3	Melt extract	
$M_o$		—	—	0	—	
$P_m$	1:0:0:0.35	22.5	0.40	3	Melt extract	
$P_o$		—	—	0	—	

under uncontrolled temperature and humidity conditions, as indicated in Table I.

Shrinkage measurements were made by means of a Demec extensometer over a gauge length of 200 mm. The first reading was taken at 24 h after casting and regular measurements were made thereafter up to 360 days age.

#### 4. Results and discussion

Some typical free shrinkage data, as obtained in this investigation, is presented and the influence of steel fibre reinforcement on this property is discussed briefly. This is followed by the determination of the coefficient of friction,  $\mu$ , of the steel fibre–cement matrix interface, using Equation 14. The  $\mu$  values thus obtained are compared with the currently available information on the frictional coefficient between steel and cement matrices and the validity of the proposed free shrinkage theory is established by this comparison. Further, the interfacial bond values,  $\tau$ , are calculated for the various fibre reinforced mixes used in this investigation by using Equations 13 and 14 and comparison made with available data for  $\tau$  as obtained from direct and indirect pull-out tests.

Finally, using the average values of  $\mu$  for individual types of fibres, and cement matrices, theoretical values of free shrinkage of fibre reinforced cement matrices are calculated using Equation 8. The theoretical and experimental results are compared to establish the validity of the proposed free shrinkage model to steel fibre reinforced cement-based materials. Finally, by adopting an empirical approach a simple design

expression for the free shrinkage of steel fibre reinforced cement matrices is derived.

#### 4.1. Influence of steel fibre reinforcement on the free shrinkage of cement matrices

The results in Figs. 4 and 5 show the relationship between age of curing and free shrinkage of some typical mixes used in this investigation. Shrinkage values at up to 360 days of age are presented. The general trend of the results is similar to the limited data available from other reports [4, 5], indicating a significant progressive reduction in shrinkage with increasing fibre content.

#### 4.2. Determination of the coefficient of friction, $\mu$

The values of the coefficient of friction,  $\mu$ , at the steel fibre–cement matrix interface are calculated from Equation 14 of the proposed theory by using the experimental data on free shrinkage obtained in this investigation. These values are determined by substituting in Equation 14 the free shrinkage strains of the control and corresponding fibre reinforced matrices at various ages of cure, namely 28, 60, 90, 120 and 180 days. The values of  $\mu$  thus obtained for the different types and volume fractions of steel fibres used to reinforce cement-paste, mortar and concrete matrices are plotted against age of cure in Fig. 6. The data are presented separately in two groups, the first group incorporating results for concrete matrices only and the second group showing the  $\mu$  values obtained for cement-paste and mortar matrices.

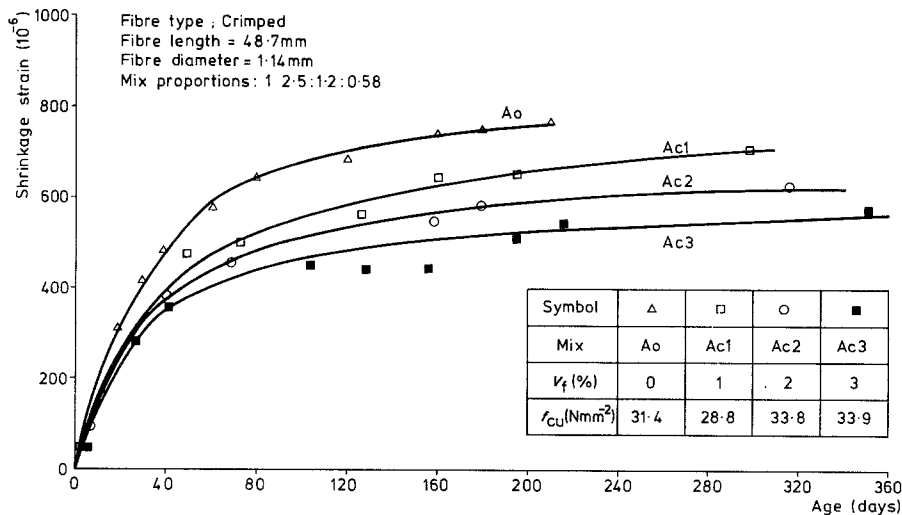


Figure 4 Influence of crimped steel fibres on the free shrinkage of concrete.

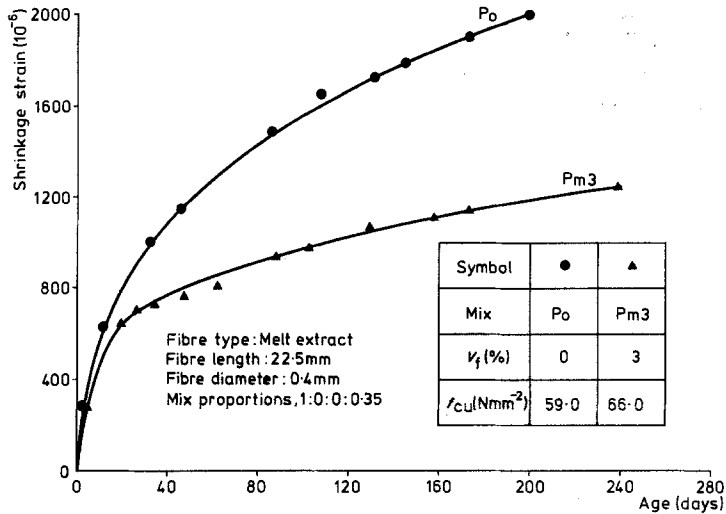


Figure 5 Influence of melt extract steel fibres on the free shrinkage of cement-paste matrices.

The  $\mu$  values for concrete matrices lie distinctly in separate bands for the three groups of fibres, namely crimped, straight, and hooked and melt extract. The band for melt extract and hooked fibres in mortar matrices is similar to the one for concrete matrices. In the case of cement-paste matrices, however, the  $\mu$  values obtained for melt extract fibres are higher than the corresponding values for concrete or mortar matrices.

It can be seen from Fig. 6 that age of curing has no significant or consistent effect on the values

of the coefficient of friction,  $\mu$ . It is also evident that the influence of fibre content on  $\mu$  is insignificant except possibly in the case of plain, straight fibres at a fibre content of 0.5 per cent. This level of fibre addition, which is too low for practical purposes, may not be truly represented by the proposed free shrinkage model, as will be discussed at a later stage.

The fact that age of curing and fibre volume fraction has no significant influence on the  $\mu$  values, leads to the conclusion that the coefficient

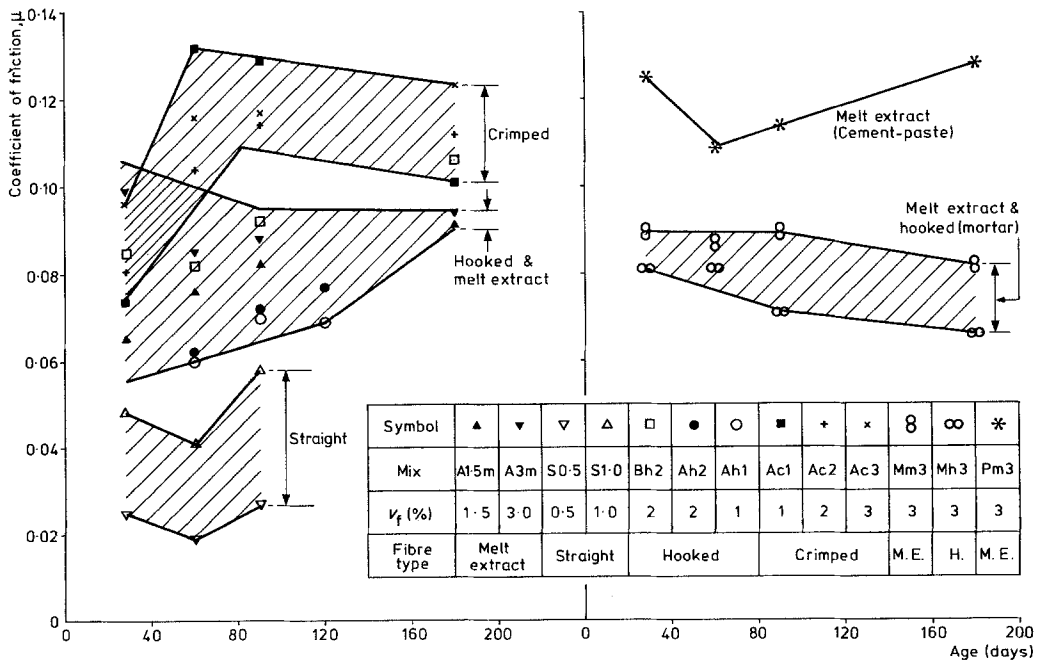


Figure 6 Effect of age and fibre volume on the coefficient of friction,  $\mu$ .

TABLE II The coefficient of friction values for different fibre types and mix proportions

Fibre type	Average coefficient of friction, $\mu$	Mix proportions
Crimped	0.11	1:2.5:1.2:0.58 (concrete matrix)
Melt extract	0.08	1:2.5:1.2:0.58 (concrete matrix)
Hooked	0.08	1:1.5:2.2:0.54 1:2.5:1.2:0.58 (concrete matrix)
Straight	0.04	1:1.18:2.25:0.42 (concrete matrix)
Melt extract	0.09	1:2.75:0:0.58 (mortar matrix)
Hooked	0.09	1:2.75:0:0.58 (mortar matrix)
Melt extract	0.12	1:0:0:0.35 (cement-paste matrix)

of friction is a material property of the fibre–matrix interface. Consequently the constituents of the matrix and surface texture and shape of steel fibres are the primary factors which govern the coefficient of friction,  $\mu$ . The average values of  $\mu$  for the three different bands established for concrete matrices and the separate bands for mortar and cement-paste, as shown in Fig. 6, are given in Table II. Considering the concrete matrices, it is evident that crimped fibres lead to the highest  $\mu$  value of 0.11 as compared to hooked, melt extract and plain steel fibres. This may be

due to the extra anchorage that these types of fibres provide. The surface roughness of melt extract fibres and the anchorage at the ends of hooked fibres lead to similar resistance to pull-out and consequently have a common  $\mu$  value in concrete of 0.08. The plain, straight fibres obviously provide minimum frictional restraint and consequently have the smallest  $\mu$  value.

The  $\mu$  value of 0.08 for hooked and melt extract steel fibres in concrete is remarkably similar to the 0.09 value obtained in mortar matrices. Cement-paste matrices however, lead to the maximum value for coefficient of friction of 0.12.

The  $\mu$  values for steel fibre–cement matrix interfaces, given in Table II, are sensibly of the same order of magnitude as the value of 0.55 recommended in CP110 for the calculation of frictional losses in pre-stressed concrete when considering steel on concrete type of contact. This similarity in  $\mu$  values obtained from entirely different approaches and assumptions is considered to lend credibility to the proposed free shrinkage model.

### 4.3. Steel fibre–cement matrix interfacial bond strength, $\tau$

Based on the average  $\mu$  values for the different groups of steel fibres and matrix constituents, as given in Table II, the average fibre–matrix interfacial bond strength,  $\tau$ , is calculated from Equation 15, the value of radial pressure,  $P$ , being determined by Equation 13.

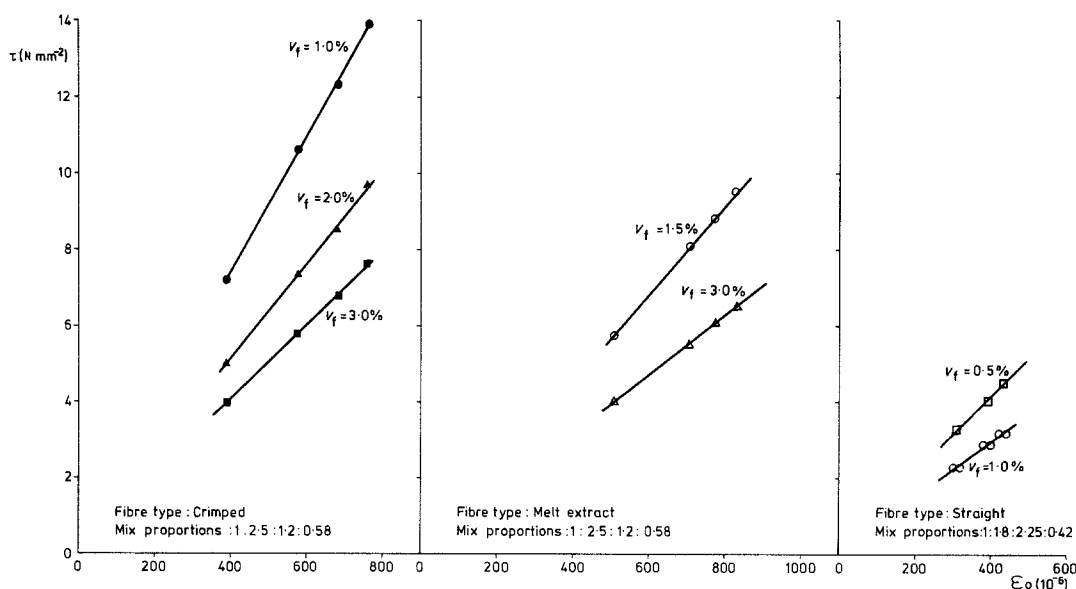


Figure 7 Influence of shrinkage and fibre volume on the fibre–matrix interfacial bond strength in concrete.

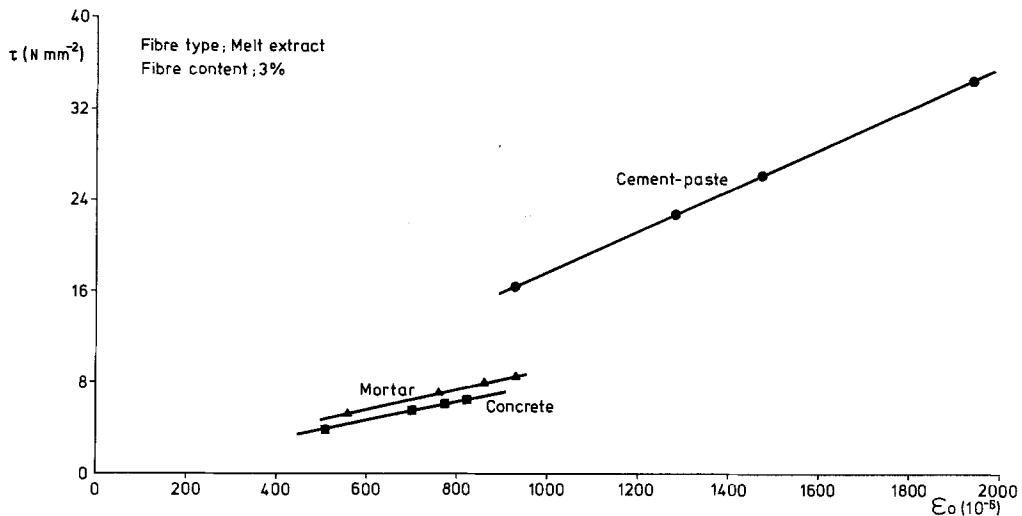


Figure 8 Effect of shrinkage and mix proportions on the fibre–matrix interfacial bond strength.

The values of  $\tau$ , as calculated from Equation 15, are plotted against the matrix shrinkage strains, caused by age of curing, in Figs. 7 and 8. In order to facilitate comparison,  $\tau$  values for different fibre types and matrices are also tabulated in Table III, at matrix shrinkage strain values of 500 and 900 microstrain.

Data pertaining to concrete matrices and the various fibre types and volume fractions used in this investigation are presented in Fig. 7. It is evident that bond strength,  $\tau$ , increases linearly with increasing shrinkage strain of the matrix,  $\epsilon_{os}$ . This is due to the form of Equation 13 which gives greater values of radial pressure,  $P$ , with increasing  $\epsilon_{os}$ .

For a constant volume fraction,  $V_f$ , of a particular fibre,  $P$  increases linearly with  $\epsilon_{os}$ . Furthermore, for a particular group of fibres and matrix, a constant  $\mu$  value is assumed in Equation 15, thus leading to a linear increase in  $\tau$  with increasing  $\epsilon_{os}$ . It is also evident from Fig. 7 that increasing

the fibre content of a mix leads to a reduction in the average interfacial bond strength,  $\tau$ . This is due to the fact that higher volume fractions of fibres lead to smaller values for fibre spacing,  $s$ , as calculated from Equation 6. This in turn decreases the cross-sectional area,  $\pi s^2/4$ , of the matrix cylinder surrounding each fibre as represented in Fig. 3. Consequently, the radial pressure,  $P$ , exerted on the surface of a fibre due to matrix shrinkage decreases with increasing  $V_f$ , thus leading to smaller  $\tau$  values.

The influence of different types of steel fibres on the values of  $\tau$  is evident from Fig. 7 and Table III. At a constant fibre content of 3 per cent in a concrete matrix, for example,  $\tau$  values are the highest for crimped fibres followed by melt extract and plain, straight fibres. This is primarily due to the shape and surface texture of these fibres.

Data at 3 per cent fibre volume for concrete, mortar and cement-paste matrices is plotted in Fig. 8. It is obvious from Fig. 8 and Table III that  $\tau$  values for mortar and concrete matrices are marginally different, whereas cement-paste matrices lead to a significantly higher bond strength. For example, considering a shrinkage strain of 900 microstrain and melt extract fibres, the  $\tau$  values reduce from 16.0 for cement-paste to 8.4 and 7.2  $\text{N mm}^{-2}$  for mortar and concrete respectively.

The  $\tau$  values obtained in this investigation range between the extremes of 2.3 and 13.9  $\text{N mm}^{-2}$  for mortar and concrete matrices. The values in cement-paste matrices are higher and range between 16.4 and 34.5  $\text{N mm}^{-2}$ . The above  $\tau$  values for mortar and concrete when compared with the

TABLE III Bond stresses for different types of steel fibres and cement-matrices at  $V_f = 3\%$

Shrinkage strain, $\epsilon_{os}$ ( $10^{-6}$ )	Matrix	Fibre type	$\tau$ ( $\text{N mm}^{-2}$ )
500	Concrete	Crimped	5.0
		Melt extract	3.9
		Plain, straight	$\leq 3.6$
	Mortar	Melt extract	4.8
900	Cement-paste	Melt extract	16.0
	Mortar		8.4
	Concrete		7.2



existing data on fibre–matrix interfacial bond [6] show reasonable agreement. For example, the values of  $\tau$  obtained from direct pull-out tests by various researchers range between 0.6 to 13.0 Nmm<sup>-2</sup> [6]. The corresponding values for flexural pull-out, obtained either indirectly from the law of mixtures expression or from flexural pull-out tests, range between 0.4 to 5.3 Nmm<sup>-2</sup> [7, 8]. The discrepancies in the  $\tau$  values obtained from the free shrinkage theory in this paper and the values obtained from direct and flexural pull-out modes are most likely to be due to the different states of stress which exist in the matrix. Despite these differences, however, the  $\tau$  values for the three types of tests are of the same order of magnitude, which lends further support to the shrinkage model proposed in this paper.

#### 4.4. Theoretical free shrinkage results for steel fibre reinforced cement matrices

Free shrinkage strains of steel fibre reinforced cement matrices can be obtained from Equation 8 based on the knowledge of the free shrinkage of the unreinforced control matrix,  $\epsilon_{os}$ . The value of fibre–matrix interfacial bond strength,  $\tau$ , is determined from Equation 15 by assuming constant frictional coefficient,  $\mu$ , values for the various types of steel fibres and matrices, as given in Table II. The interfacial pressure on the fibre sur-

face is determined from Equation 13. The remaining parameters in Equation 8 are functions of fibre geometry, fibre volume fraction and the stress–strain characteristics of the control matrix, which can be easily determined.

Some typical theoretical free shrinkage results for steel fibre reinforced cement matrices, as obtained from Equation 8 are presented in Fig. 9 along with the corresponding experimental data. The graphs represent three types of materials, namely cement-paste reinforced with 3 per cent melt extract fibres, mortar matrices reinforced with 3 per cent hooked fibres and concrete matrices reinforced with 3 per cent crimped fibres. It is obvious that the correlation between experimental and theoretical results is very close.

#### 5. Design expression for shrinkage of steel fibre reinforced cement matrices

Although the free shrinkage of steel fibre reinforced cement based matrices is predicted satisfactorily by Equation 8 of the proposed theory, it is desirable to obtain a simple design expression for this property. It is found that there exists a linear relationship between the free shrinkage of steel fibre reinforced matrices,  $\epsilon_{fs}$ , and the corresponding shrinkage of control cement matrices,  $\epsilon_{os}$ , as indicated in Figs. 10 and 11 which represent some typical examples of the results obtained

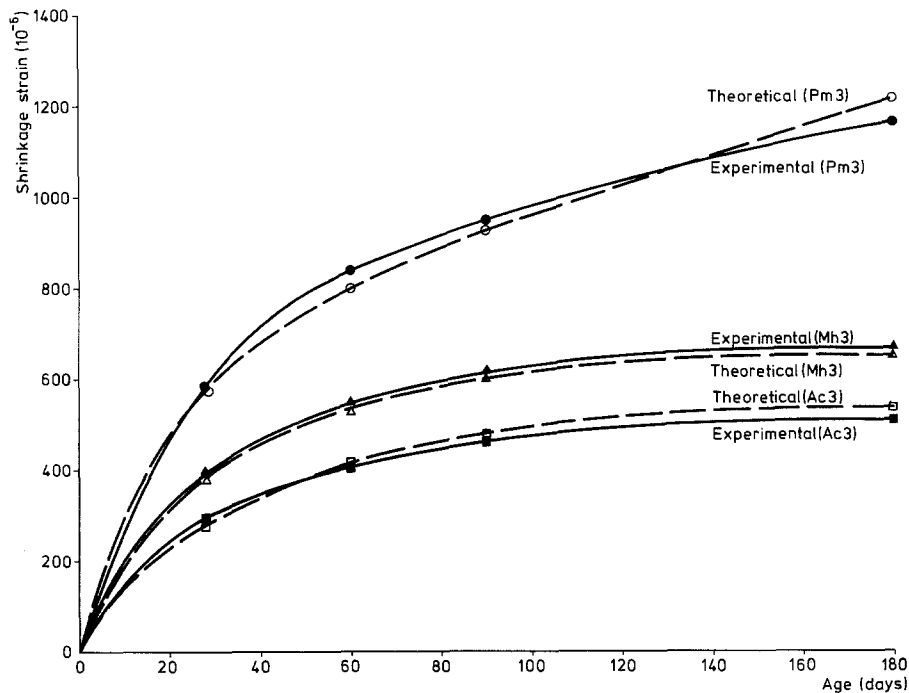


Figure 9 Comparison between theoretical and experimental results.

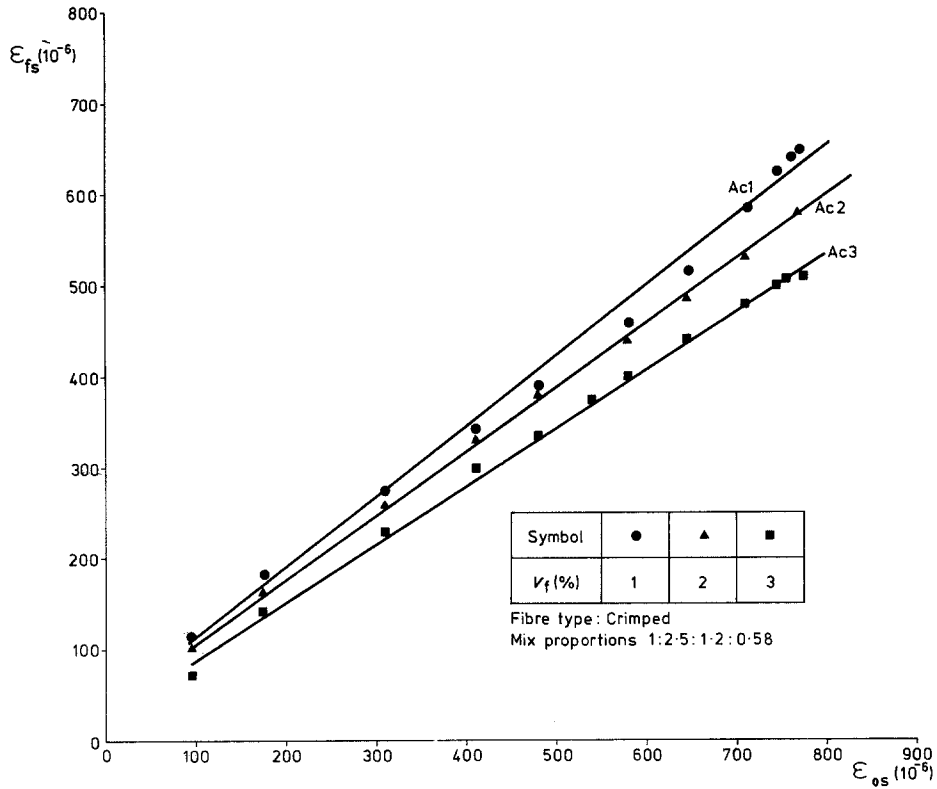


Figure 10 Relationship between the free shrinkage of control and fibre reinforced concrete.

in this investigation. From these results, it follows that:

$$\epsilon_{fs} = m\epsilon_{os} \quad (16)$$

where  $m$  is the slope of the graphs between  $\epsilon_{os}$  and  $\epsilon_{fs}$ .

The slope  $m$  becomes progressively less as the fibre content increases, thus indicating that the reduction in shrinkage due to fibre reinforcement is a function of  $m$ . Furthermore, the values of  $m$  can be related to  $\mu V_f l/d$ , as shown in Fig. 12, leading to the following relationship:

$$m = -5.71\mu V_f \frac{l}{d} + 1 \quad \text{for } \mu V_f \frac{l}{d} < 0.038 \quad (17)$$

$$m = -1.23\mu V_f \frac{l}{d} + 0.84 \quad \text{for } \mu V_f \frac{l}{d} > 0.038 \quad (18)$$

Substituting the  $m$  values from Equations 17 and 18 into Equation 16 leads to the following design

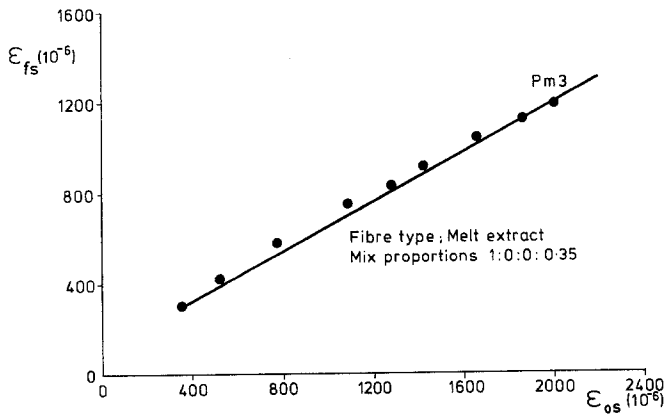


Figure 11 Relationship between the free shrinkage of control and fibre reinforced cement-paste.

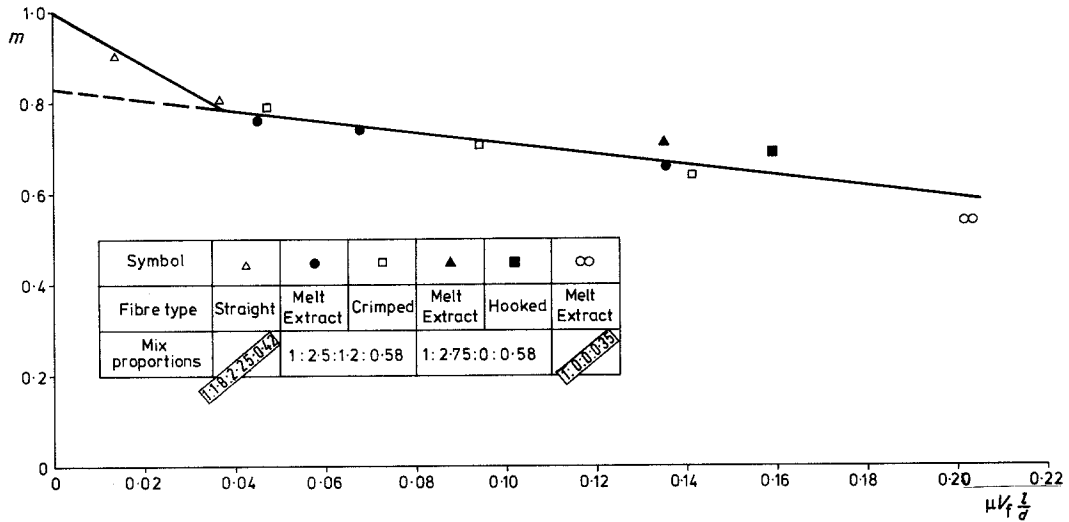


Figure 12 Relationship between  $m$  and  $\mu V_f l/d$  for fibre-reinforced concrete, mortar and cement paste.

expressions for the shrinkage of steel fibre reinforced cement matrices:

$$\epsilon_{fs} = \epsilon_{os} \left( 1 - 5.71 \mu V_f \frac{l}{d} \right) \quad \text{for } \mu V_f \frac{l}{d} < 0.038 \quad (19)$$

and

$$\epsilon_{fs} = \epsilon_{os} \left( 0.84 - 1.23 \mu V_f \frac{l}{d} \right) \quad \text{for } \mu V_f \frac{l}{d} > 0.038 \quad (20)$$

The shrinkage of steel fibre reinforced matrices can be obtained simply from the above equations, based on the knowledge of the free shrinkage of unreinforced cement matrices and the volume fraction and properties of steel fibres.

An important fact which emerges from Fig. 12 is that the mechanism of shrinkage restraint provided by steel fibres changes at  $\mu V_f l/d$  values of under 0.038. This fact is further confirmed by the unexpectedly low  $\mu$  values, as seen in Fig. 10, for straight, plain fibres at a fibre content of 0.5 per cent. The fact that small  $\mu V_f l/d$  values of less than 0.038 are only possible for very small values of  $V_f$  or  $l/d$ , which seldom occur in practice, implies that only Equation 20 is important for design purposes.

## 6. Conclusions

The free shrinkage model for randomly oriented steel fibres in a cement based matrix, which considers the shrinkage of a thick cylinder of the matrix being restrained by an equivalent length of an aligned fibre, has been shown to be valid.

The coefficient of friction at the fibre–matrix interface,  $\mu$ , is affected primarily by the constituents of the matrix and shape and surface texture of the steel fibres. The values obtained range between 0.04 and 0.12. Generally rough or mechanically deformed fibres lead to higher  $\mu$  values. Cement-paste matrices lead to higher  $\mu$  values than concrete or mortar.

The steel fibre–cement matrix interfacial bond strength,  $\tau$ , is primarily a function of the shrinkage strain in the matrix. Other important factors are fibre volume fraction and matrix constituents. Increasing fibre contents lead to a reduction in  $\tau$  values. Cement-paste matrices yield greater  $\tau$  values than mortar or concrete matrices. Depending on the matrix shrinkage strain, values of  $\tau$  for cement matrices range between 16 and 34.5 N mm<sup>-2</sup>, whereas for the mortar and concrete the range is between 2.3 and 13.9 N mm<sup>-2</sup>.

For most practical purposes, a simple empirical expression of the form

$$\epsilon_{fs} = \epsilon_{os} \left( 0.84 - 1.23 \mu V_f \frac{l}{d} \right)$$

can be used to predict the free shrinkage,  $\epsilon_{fs}$ , of fibre reinforced cement matrices based on the control shrinkage,  $\epsilon_{os}$ , and fibre properties.

## Acknowledgements

The authors gratefully acknowledge the support of the Science and Engineering Research Council, UK for this work, which is part of a larger study on steel fibre reinforced cement matrices.

## References

1. G. PICKETT, *A.C.I.* 52 (1956) 581.
2. J. P. ROMUALDI and J. A. MANDEL, *A.C.I.* 61 (1964) 647.
3. S. TIMOSHENKO, "Strength of Materials", Part II, Advanced Theory and Problems, 3rd edn. (Van Nostrand Co. Inc., New York, 1956) p. 205.
4. R. N. SWAMY and H. STAVRIDES, *A.C.I.* 75 (1979) 443.
5. B. MALMBERG and A. SKARENDAHL, Fibre Betong, Nordforsks Projekt Komitee for FRC material, Stockholm (1979) p. 1.
6. P. BARTOS, *Int. J. Cement Composites and Lightweight Concrete* 3 (1981) 159.
7. R. N. SWAMY and P. S. MANGAT, *Cement and Concrete Res.* 6 (1976) 641.
8. P. S. MANGAT, M. MOTAMED AZARI and B. B. SHAKOR RAMAT, *Int. J. Cement Composites and Lightweight Concrete* 5 (1983) 4.

*Received 16 September  
and accepted 29 September 1983*